Final Report

Multiscale Lightning Data Assimilation for Improved Weather and Air Quality Modeling

TCEQ Contract No. 582-19-90498
Work Order No. **582-22-31297-009**

Deliverable 8.2
Revision 2.0

Prepared by:

Rebecca Adams-Selin, Jennifer Hegarty, Rick Pernak, Eric Fanny, and Matthew Alvarado
Atmospheric and Environmental Research, Inc. (AER)
131 Hartwell Ave.
Lexington, MA 02421
Correspondence to: rselin@aer.com

Prepared for:

Peter Hoholick
Texas Commission on Environmental Quality (TCEQ)
Air Quality Division
Building E, Room 318
Austin, Texas 78711-3087

30 June 2022

Document Change Record

Revision	Revision Date	Remarks
0.1	**21 June 2022**	**Internal Version for Review**
1.0	**21 June 2022**	**Delivery to TCEQ**
1.5	**29June 2022**	**Internal Version for Review**
2.0	**30 June 2022**	**Delivery to TCEQ**

TABLE OF CONTENTS

1 Introduction 6
1.1 Project Objectives 6
1.2 Background 6
2 Lightning Data Assimilation 6
2.1 GLM Data 6
2.2 Preprocessing and Regridding GLM data 7
2.3 Quality assurance of regridded GLM data 8
2.4 Lightning Data Assimilation Options in WRF MSKF 8
2.5 Impact of MSKF Suppression Options 8
3 Evaluation of WRF Runs with and without LDA 11
3.1 Using MET 11
3.2 Temperature and Winds 11
3.3 Evaluating 6 and 24-hour Precipitation 13
3.4 Explanation for lack of Impact of LDA on Statistics 16
4 Impact of LDA on CAMx 19
4.1 Description of CAMx 19
4.2 Evaluation of CAMx with and without WRF LDA 19
5 Summary and Recommendations for Further Study 21
6 References 22

LIST OF FIGURES

Figure 1: (a) The LNT field for a 24-hour WRF-MSKF-LDA simulation beginning 0000 UTC 1 June 2019. The red shaded areas are grid points for which lightning was observed during the simulation period. (b) RAINC field accumulation ending at 0000 UTC 2 June 2019. This simulation was performed with suppress_opt=2. (c) RAINC field accumulation ending at 0000 UTC 2 June 2019 with suppress_opt=0. (d) Accumulated 24-h precipitation from the NCEP/EMC Stage-IV gridded analysis over the same time period. The Stage-IV analysis uses a radar-based precipitation estimate that is manually quality controlled using surface observation data. 10

Figure 2: 24-hour Gridded and convective precipitation for the June 6, 2019 case fro WRF LDA (top) and WRF_noLDA (bottom) 15

Figure 3: (upper left) WRF accumulated RAINC in LDA run (mm; colorbar) and occurrence of lightning in WRF grid cell (pink dots) over 24 h ending 0600 UTC 7 June 2019. (upper right) WRF accumulated RAINC in noLDA run (mm; colorbar). (bottom left) Difference between RAINC in LDA – noLDA run. Brown regions are where the LDA run was drier than the noLDA run. (bottom right) Stage-IV precipitation analysis. Note the different color scale used. 17

Figure 4: As in Fig. 2, but for RAINNC, gird-scale precipitation. Note the precipitation color scales for WRF RAINNC and Stage-IV are now similar. 18

Figure 5. Scatterplots of MDA8 values for all days and sites in East Texas for June 2019. (a) a) CAMx simulation with LDA. (b) CAMx simulation without LDA. 20

Figure 6. Mean bias in MDA8 O3 for June 2019 at all AQS sites in East Texas. (a) CAMx simulation with LDA. (b) CAMx simulation without LDA. 21

LIST OF TABLES

Table 1: WRF MET temperature statistics for the simulations with and without LDA. 11

Table 2: U wind speed statistics..... 12

Table 3: V wind speed statistics..... 12

Table 4: WRF MET precipitation statistics for the simulations with and without LDA. 14

Table 5. Statistics for MDA8 O_3 across all sites in East Texas for June 2019. 20

Executive Summary

The purpose of this project is to improve TCEQ's simulation of ozone photochemistry by applying a proven lightning data assimilation (LDA) method in the Weather Research and Forecasting (WRF) model. The method will force deep convection in the meteorological model where lightning is observed and only allow shallow convection where it is not, which will improve the representation of clouds in the meteorological and photochemical models. This is accomplished in WRF through the Multi-Scale Kain Fritsch (MSKF) cumulus parameterization scheme (Zheng et al., 2016) and the version of WRF with this capability is referred to here as WRF-MSKF-LDA.

In this work, AER developed software to download, process, and regrid publicly available observations from the Geostationary Lightning Mapper (GLM) into the input format required by the WRF LDA method. A User's Guide was provided to TCEQ for this software. To determine the accuracy of the lightning regridding software, we (1) used multiple calculation methods to determine the WRF grid point nearest a flash and (2) plotted comparisons of multiple time periods of raw flash data and regridded data (LNT). The resulting LNT data, regridded using both methods, were identical for all tested dates. Plots of co-located raw flash and regridded lightning data were also used for evaluation over different time scales (multiple days, multiple hours, only 10 minutes).

We implemented the LDA method into the MSKF scheme in WRF and provided TCEQ with a recipe to implement this change in current and future versions of WRF. We evaluated the performance of WRF for June 2019 simulations with the Model Evaluation Toolkit (MET). The domain and namelist configuration of the WRF run were provided directly by TCEQ. Per the work order, we performed point-based verification of temperature and wind speed by comparing WRF output to surface station observations obtained from MADIS. We also performed grid-based verification of precipitation by comparing WRF output to Stage-IV radar-based precipitation estimates. Stage-IV precipitation data was accumulated over 24-h and 6-h intervals. We found little difference in the temperature, wind, and precipitation verification across both domains, which was highly surprising. Evaluation revealed that the LDA worked almost solely to suppress precipitation where lightning did not occur and was not adding precipitation where lightning was occurring. We theorize increasing the perturbation threshold LDA allows inside the MSKF to trigger convection could address this issue.

To test the impact of the new MSKF LDA data assimilation on simulations of O_3 in Texas, we ran CAMx with (LDA) and without LDA (noLDA) for June 2019. CAMx inputs for May 15-June 30 were provided by TCEQ corresponding to their 2019 O_3 modeling platform. In general, both CAMx runs compare well to observations, with low mean bias and mean error. However, there is little difference between the noLDA and LDA runs, and to the extent there is a difference, the noLDA runs are slightly worse. For example, the mean bias across all East Texas sites and days increased to 2.5 ppbv from 2.2 ppbv when LDA was implemented.

For future work, we recommend testing an increase in the moisture and temperature perturbations allowed within LDA for triggering convection in MSKF. This increase is necessary due to the different way entrainment and convective updraft is calculated within MSKF compared to the Kain-Fritsch (KF, Kain, 2004), parameterizations, where LDA was originally implemented and tested.

1 Introduction

1.1 Project Objectives

The purpose of this project is to improve TCEQ's simulation of ozone photochemistry by applying a proven lightning data assimilation (LDA) method in the Weather Research and Forecasting (WRF) model. The method will force deep convection in the meteorological model where lightning is observed and only allow shallow convection where it is not, which will improve the representation of clouds in the meteorological and photochemical models. This is accomplished in WRF through the Multi-Scale Kain Fritsch (MSKF) cumulus parameterization scheme (Zheng et al., 2016) and the version of WRF with this capability is referred to here as WRF-MSKF-LDA.

1.2 Background

A key deficiency of many retrospective meteorological simulations is the timing and location of convective rainfall. In addition to poor simulation of rainfall itself, misplacement of deep convection can negatively affect near-surface meteorology such as temperature, humidity, winds, and boundary layer height, all of which negatively impact air quality simulations.

Heath et al., (2016) developed a simple LDA method for improving parameterized deep convection in retrospective weather simulations. The method has a straightforward approach to force deep convection where lightning is observed and only allow shallow convection where it is not. The LDA method has been used to improve air quality simulations in Community Model for Air Quality (CMAQ) (Heath et al. 2018) and into the modeling system used by the Environmental Protection Agency (EPA) (e.g., Kang et al., 2020; Pleim et al., 2019; Kang et al. 2019; Pye et al., 2018; Foroutan and Pleim, 2017). The LDA method for this project improves upon the previous work by applying the technique at higher resolutions and using publicly available satellite-derived lightning observations from GLM (Goodman et al., 2013).

2 Lightning Data Assimilation

A LDA User Guide document, Deliverables 3.2 and 4.2, describes the code provided by AER to download, process, and regrid publicly available observations from the Geostationary Lightning Mapper (GLM) into the input format required by the WRF LDA method. It consists of three Python scripts: get_data.py, to retrieve the data; regrid_ltg.py, to regrid the data to the WRF grid; and gcdistance.py, a function called by regrid_ltg.py. Methods for installing the libraries necessary to run the codes on TCEQ computing systems were included in the User Guide, along with quality assurance of the gridded lightning data when compared to the point lightning flash data.

2.1 GLM Data

The get_data.py script, executed with two arguments, start_date and end_date, will download all the GLM data between (and inclusive of) those dates. The data files will be downloaded in netCDF format to sub-directories with names corresponding to the day-of-year and hour of the data. For example, the data for June 1, 2019, for 0000 UTC to 0059 UTC will be downloaded to sub-directory 152/00. Each file will have a descriptive name that indicates the range of the time covered and the creation date. For example, the file name below can be interpreted as follows.
OR_GLM-L2-LCFA_G16_s20191520000000_e20191520000200_c20191520000228.nc

Data starting date: 2019 day 152

Data starting time: 00:00:00.0 UTC

Data starting date: 2019 day 152

Data ending time: 00:00:20.0 UTC

File creation date: 2019 day 152

File creation time: 00:00:22.8 UTC

The file sizes are variable depending on how much lightning data is available. Generally, we have found that 1 day is about 1.5 – 2.5 GB of data.

2.2 Preprocessing and Regridding GLM data

The lightning data is then regridded to the WRF domain using regrid_ltg.py. The script requires that the GLM data have been downloaded into the directory structure described in the previous section. It also needs WRF grid information from the geo_em.d{*domid*}.nc file that is created by the WPS. Finally, it also requires the gcdistance function and expects it to be available via the delivered gcdistance.py file placed in the same working directory. The command syntax for regrid_ltg.py is illustrated with the following example.

```
python regrid_ltg.py --start_date 2019-06-01_00:00:00 --
end_date 2019-06-02_00:00:00 --base_dir /mnt/fsx-
rd/WRF_LDA/GLM_Data --wrf_dir /mnt/fsx-rd/WRF_LDA/WPS --
domid 01
```

In the above example note that *start_date* and *end_date* inputs include the hours, minutes, and seconds. These parameters must be specified to exactly match the start and end times of the WRF run. The *base_dir* parameter must include the full path to the GLM data where there will be day-of-year/hour subdirectories as described in the previous section. Similarly, the *wrf_dir* input must include the full path to the WRF geo_em.d{*domid*}.nc file. The *domid* input specifies to which WRF domain the lightning data will be regridded.

The output of the script is one ltgda_d{*domid*}_YYYY-MM-DD.nc file with YYYY-MM-DD corresponding to *start_date*. The file contains one variable, LNT, of the same horizontal dimensions as the WRF domain *domid*, with the grid cell set to 1 if a lightning flash occurred within that cell and 0 if not. LNT also has a time dimension that currently updates at 10 min timesteps. Each LNT timestep includes any lightning flash occurrences between that time and 30 min into the future. The 10-min update cadence and 30-min accumulation interval was chosen to coincide with Heath et al. (2016) and its original development of the lightning data assimilation method. The inclusion of 30 minutes into the future at each timestep allows the convective parameterization to be turned on prior to the appearance of lightning, as convection typically initiates some time before the first lightning flash. The 10-min update cadence will be tested during upcoming tasks to evaluate the sensitivity of the LDA method to that selection.

The current configuration of one output file containing all timesteps can be modified by AER upon request if the size of the file becomes unwieldy: if a ltgda file is being created for a WRF run lasting for several months, for example. In the case of the WRF runs conducted as described below, one ltgda file was created for each domain for each day's run (30 hours), which were all initialized individually.

2.3 Quality assurance of regridded GLM data

To determine the accuracy of the lightning regridding software, we (1) used multiple calculation methods to determine the WRF grid point nearest a flash and (2) plotted comparisons of multiple time periods of raw flash data and regridded data (LNT). The two calculation methods used were the geopy library distance function and an internally coded great circle distance function using the haversine formula; the two methods assume slightly different shapes of the earth. The resulting LNT data, regridded using both methods, were identical for all tested dates. Plots of co-located raw flash and regridded lightning data were also used for evaluation over different time scales (multiple days, multiple hours, only 10 minutes). Again, all were identical.

2.4 Lightning Data Assimilation Options in WRF MSKF

There are several options that control the lightning data assimilation in the WRF-MSKF-LDA system. One is the time interval at which lightning data will be simulated. This is determined by generating gridded lightning data at a specified time interval and specifying this same interval in the WRF namelist.input file as described in the Technical Memo for Deliverable 5.1 An interval of 10 minutes is recommended as this has been tested in the development of the assimilation system (Heath et al., 2016) and is the interval used in the simulations performed for this project. In practice, the advantages of a shorter time interval must be weighed against the disadvantages of increased compute time and storage space required for the gridded lighting data files. Another option that can influence the impact of the LDA is the interval at which the MSKF convective scheme is called. Generally, the cumulus parameterization interval, *cudt*, set in namelist.input should be set to 0, to run every model timestep. The WRF run time can be sped up, slightly, by setting it to 10 to match the grouping of the lightning observations. As with the lightning data interval there will be a trade-off between model compute time and simulation accuracy.

There are also three convection suppression options available in the WRF-MSKF-LDA system and these are set with the *suppress_opt* entry in the WRF namelist.input file as described in the Technical Memo for Deliverable 5.1. If *suppress_opt*=0, the MSKF scheme will run as normal if lightning is not present in a grid box, but deep convection will be forced if the lightning is present. For *suppress_opt=1*, if lightning is not present in a grid box the MSKF scheme will be skipped entirely. This option is generally not recommended as it is the most severe restriction on convective parameterization. For *suppress_opt=2*, if lightning is not present only shallow convection will be allowed in the MSKF scheme. Some tests at EPA (Heath et al., 2016) showed that *suppress_opt=2* was the best option for the normal KF scheme (Kain, 2004), thus, this is the recommended starting option. But option *suppress_opt=0* may also work well for the MSKF scheme, so it is worth testing if there are not major improvements with *suppress_opt=2*.

2.5 Impact of MSKF Suppression Options

A few preliminary tests were performed with the WRF-MSKF-LDA system to ensure that the lightning data were read-in correctly and that the lightning variable LNT generally lines up with convective rainfall variable RAINC in the WRF output files. These tests were also evaluated to examine the impact of the MSKF suppression options. Only *suppress_opt=0* and *suppress_opt=2* were tested. Figure 1 below shows the LNT field and Figure 1b shows the RAINC field for a 24-hour test simulation performed using suppress_opt=2, as set in the provided *namelist.input* file. Figure 1c shows the RAINC field at the same time for a simulation that was performed with all

the same settings as in Figure 2 but with suppress_opt=0. Note that for the run with the suppress_opt=2 there is a notably better match between the LNT and RAINC. It is not a perfect match because shallow RAINC as well as grid-resolved precipitation will still be included, and because the lifetime of the convective clouds is different than the grouping of the lightning observations. The suppress_opt=2 run shown in Figure 2 is also more like the observed Stage-IV precipitation analysis shown in Figure 1d. By limiting the amount of deep convection triggered by the convective parameterization, the deep convection that is triggered has a better source of available instability and can produce more intense convection and rainfall.

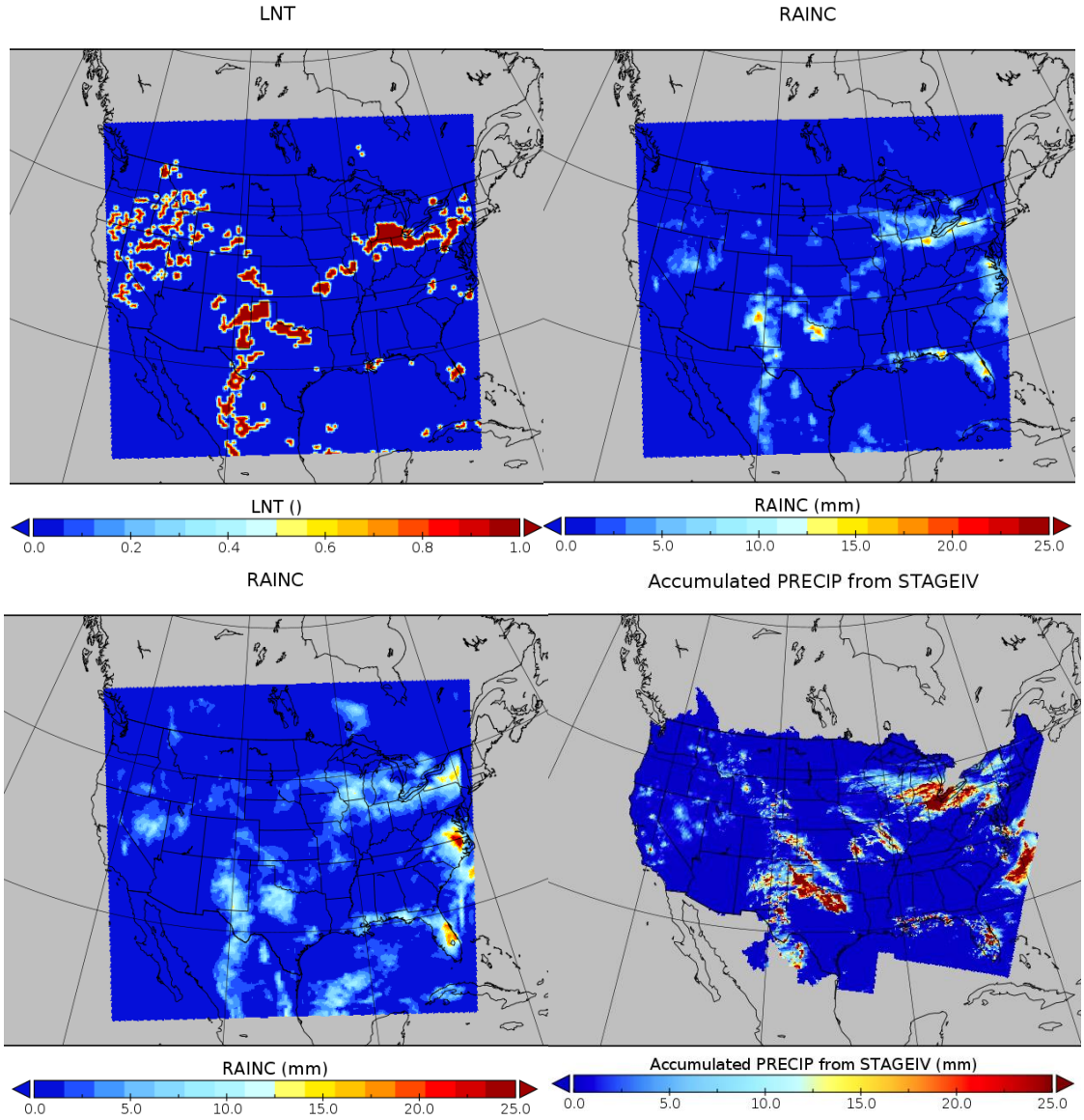

Figure 1: (a) The LNT field for a 24-hour WRF-MSKF-LDA simulation beginning 0000 UTC 1 June 2019. The red shaded areas are grid points for which lightning was observed during the simulation period. (b) RAINC field accumulation ending at 0000 UTC 2 June 2019. This simulation was performed with suppress_opt=2. (c) RAINC field accumulation ending at 0000 UTC 2 June 2019 with suppress_opt=0. (d) Accumulated 24-h precipitation from the NCEP/EMC Stage-IV gridded analysis over the same time period. The Stage-IV analysis uses a radar-based precipitation estimate that is manually quality controlled using surface observation data.

3 Evaluation of WRF Runs with and without LDA

3.1 Using MET

The Model Evaluation Toolkit (MET; available publicly online via https://dtcenter.org/community-code/model-evaluation-tools-met/download), was used to perform the WRF output validation. MET offers many different verification methods. Per the work order, we performed point-based verification of temperature and wind speed by comparing WRF output to surface station observations obtained from MADIS. Hourly observation data was retrieved. Observations within 5 minutes of the model output time were retained.

We also performed grid-based verification of precipitation by comparing WRF output to Stage-IV radar-based precipitation estimates. Stage-IV precipitation data was accumulated over 24-h intervals.

3.2 Temperature and Winds

The verification statistics for temperature are found in Table 1 and for U (west -to-east) and V (south-to-north) winds in Tables 2 and 3 respectively. Lower and upper confidence limits are calculated assuming a bivariate normal distribution of the two fields (forecast and observations). These confidence limits were used to identify statistically significant difference between the two skill scores. There were no statistically significant differences in verification statistics between the LDA and noLDA runs found for 2-m temperature or 10-m U or V wind speeds.

Table 1: WRF MET temperature statistics for the simulations with and without LDA.

Domain 1	**LDA**	**noLDA**
Pearson Correlation Coefficient	0.897494	0.895109
lower confidence limit	0.88883	0.886265
upper confidence limit	0.905519	0.903306
Mean Error	-0.005814	0.014493
lower confidence limit	-0.11081	-0.090706
upper confidence limit	0.099182	0.119693
Error Standard Deviation	2.435534	2.440162
lower confidence limit	2.36349	2.367978
upper confidence limit	2.512142	2.516918

Domain 2	**LDA**	**noLDA**
Pearson Correlation Coefficient	0.656352	0.651841
lower confidence limit	0.579312	0.57447
upper confidence limit	0.722439	0.718396
Mean Error	0.279499	0.41105
lower confidence limit	0.024556	0.159513
upper confidence limit	0.534441	0.662588
Error Standard Deviation	1.884298	1.858283
lower confidence limit	1.719612	1.695803
upper confidence limit	2.084156	2.055482

Table 2: U wind speed statistics.

Domain 1	LDA	noLDA
Pearson Correlation Coefficient	0.632422	0.643467
lower confidence limit	0.605726	0.61737
upper confidence limit	0.65771	0.668166
Mean Error	0.144268	0.127233
lower confidence limit	0.048594	0.034334
upper confidence limit	0.239942	0.220131
Error Standard Deviation	2.18067	2.117155
lower confidence limit	2.115056	2.053445
upper confidence limit	2.250516	2.184975

Domain 2	LDA	noLDA
Pearson Correlation Coefficient	0.443159	0.464456
lower confidence limit	0.330607	0.354102
upper confidence limit	0.54364	0.562392
Mean Error	0.140278	0.065772
lower confidence limit	-0.120094	-0.179684
upper confidence limit	0.400649	0.311228
Error Standard Deviation	1.899931	1.790332
lower confidence limit	1.731923	1.631955
upper confidence limit	2.10434	1.983041

Table 3: V wind speed statistics.

Domain 1	LDA	noLDA
Pearson Correlation Coefficient	0.649082	0.663419
lower confidence limit	0.623478	0.63861
upper confidence limit	0.673317	0.686872
Mean Error	0.146229	0.15806
lower confidence limit	0.045048	0.05993
upper confidence limit	0.24741	0.25619
Error Standard Deviation	2.306602	2.236837
lower confidence limit	2.237211	2.169539
upper confidence limit	2.380467	2.308476

Domain 2	LDA	noLDA
Pearson Correlation Coefficient	0.463447	0.47852

lower confidence limit	0.35541	0.371973
upper confidence limit	0.559862	0.573216
Mean Error	0.401154	0.410009
lower confidence limit	0.100074	0.126057
upper confidence limit	0.702234	0.693962
Error Standard Deviation	2.198002	2.072212
lower confidence limit	2.003719	1.888986
upper confidence limit	2.434358	2.295131

3.3 Evaluating 6 and 24-hour Precipitation

The precipitation statistics are presented in Table 4. When all thirty days of the simulation period are considered the differences between the LDA and noLDA statistics are small. We also considered whether LDA would be more impactful on days with substantial precipitation than on days where little to no precipitation occurred. For Domain 1, which covers CONUS, it was not practical to subjectively separate high precipitation days from low precipitation days as substantial precipitation occurred in some part of the domain on all the days. Therefore, we focused on Domain 2 that covered eastern Texas only, but this was also not easy as June 2019 was a very rainy month in Texas. According to NWS Advanced Hydrologic Prediction Service (AHPS) at https://water.weather.gov/precip/ many locations in eastern Texas reported more than 127 mm (5 inches) of rainfall during the month. We used daily AHPS observed precipitation analyses to select six days (20 % of total) with substantial heavy precipitation coverage and six days with little precipitation in eastern Texas. The statistics for these subsets of days are referred to in the tables as "wet" and "dry' respectively. For the wet days the Pearson Correlation Coefficient for the 24-hour precipitation was better for LDA (0.417) than for no LDA(0.312). For the 6-hour precipitation it was also better for LDA (0.238) compared to noLDA (0.210) but to a much smaller degree than for the 24-hour precipitation. However, for both the 24-hour and 6-hour precipitation the Mean Error and Standard Deviation statistics were larger for the LDA simulations. For the dry days the Pearson Correlation Coefficient for the 24-hour precipitation was greater for the LDA (0.271) than for noLDA (0.195) but for the 6-hour precipitation the LDA value (0.098) was slightly lower than for the noLDA value (0.105). However, for these days both the 24-hour and 6-hour Mean Error were about half as large for LDA than for noLDA.

Overall, the impacts of LDA on the WRF precipitation simulation were mixed and less substantial than anticipated. To investigate this further we have examined plots of convective and gridded rain for the WRF runs with and without LDA. Sample plots for the case of June 6, 2019, are shown in Figures 2. In general, it appears the lightning assimilation is significantly suppressing the convective precipitation. This possibility will be further explored in Section 3.4.

Table 4: WRF MET precipitation statistics for the simulations with and without LDA.

Domain 1	**LDA**	**noLDA**
Pearson Correlation Coefficient		
24-hour	0. 401564	0.413194
6-hour	0.290604	0.287735
Mean Error		
24-hour	0.200166	-0.188526
6-hour	0.047263	-0.042505
Error Standard Deviation		
24-hour	10.680689	9.258428
6-hour	4.950240	4.410723

Domain 2	**LDA All**	**LDA Dry**	**LDA Wet**	**noLDA All**	**noLDA Dry**	**noLDA Wet**
Pearson Correlation Coefficient						
24-hour	0.296738	0.270708	0.417221	0.257560	0.194789	0.312253
6-hour	0.153928	0.097543	0.238339	0.151281	0.105681	0.209951
Mean Error						
24-hour	0.310334	-0.971195	1.856453	-0.903175	-1.859827	0.347953
6-hour	0.082687	0.051284	0.537450	-0.228820	-0.116058	-0.295021
Error Standard Deviation						
24-hour	13.480625	9.237843	17.567272	12.58414	9.647536	17.489318

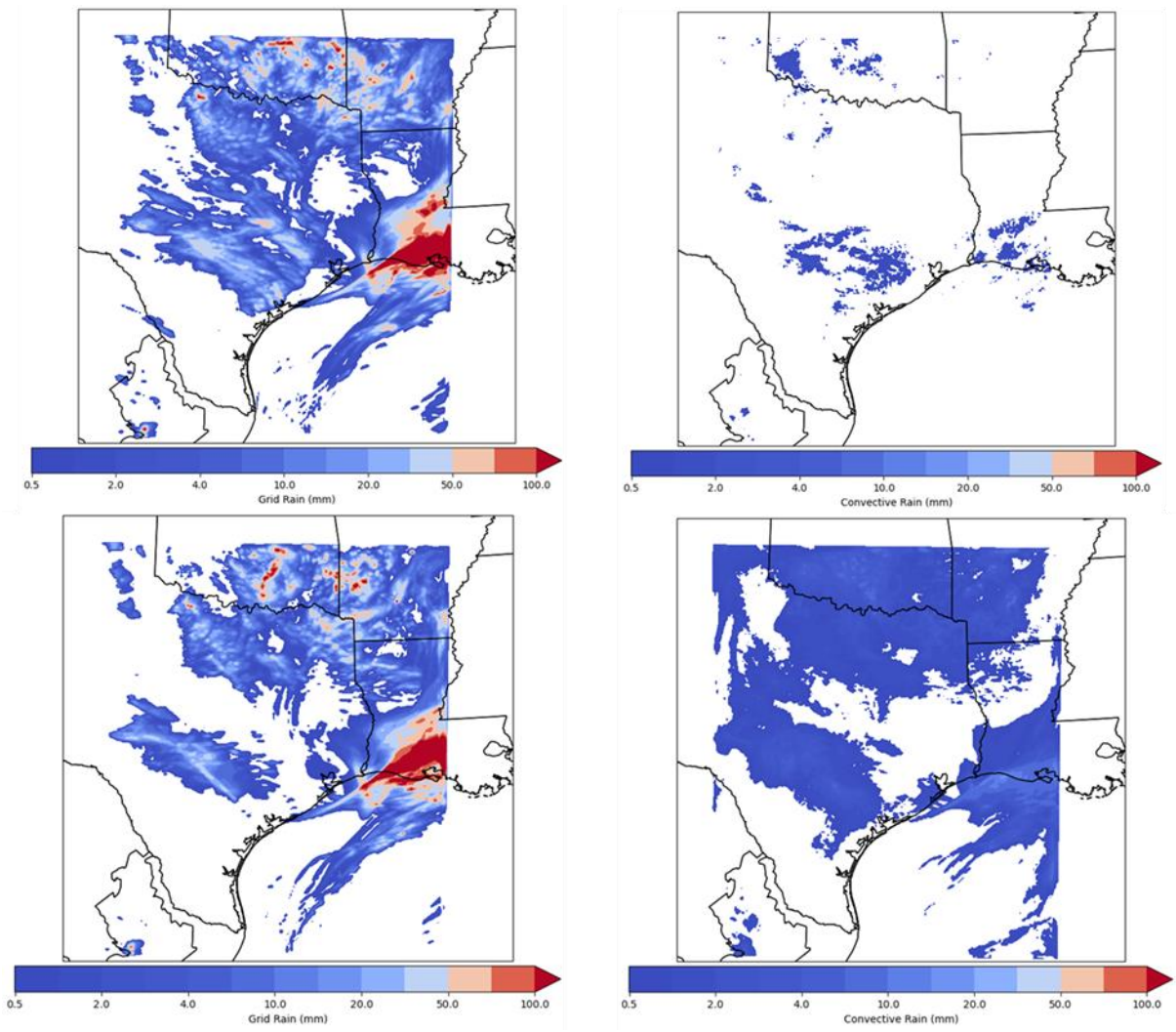

Figure 2: 24-hour Gridded and convective precipitation for the June 6, 2019 case for WRF LDA (top) and WRF_noLDA (bottom)

3.4 Explanation for lack of Impact of LDA on Statistics

The lack of impact of the LDA on the precipitation, temperature, and wind statistics was perplexing, given that we have seen extensive improvement when using the LDA method with the original Kain-Fritsch (KF) parameterization (Kain 2004): for example, in Heath et al. (2016), the original motivation for the study, as well as in recent AER work evaluating Kain-Fritsch parameterization performance both with and without LDA over the state of Oklahoma during the Deep Convective Cloud and Chemistry (DC3) field campaign, also for a domain with 12-km horizontal resolution.

To determine the reason behind this puzzling lack of impact, we evaluated the rainfall fields produced on individual dates identified as "wet" (see Section 3.1 above). The KF parameterization separates rainfall output into "RAINC", or convective precipitation output by the parameterization, and "RAINNC", or grid-scale precipitation output directly by the model itself.

Figure 3 below shows the RAINC output from WRF with LDA (upper left), without LDA (upper right), the difference between the two (bottom left), and Stage-IV observations for 6 June 2019. Note that the lower left subfigure in Figure 3 shows the impact of the LDA was almost entirely to reduce the amount of precipitation produced by the convective parameterization. Recall that suppress_opt = 2 was used, which shifts processing within the convective parameterization to the shallow part of the parameterization scheme if lightning is not detected and is then output in the grid-scale precipitation if any is produced. The suppression took place in the correct location when compared to the location of lightning (Figure 3 top left). For example, the large amount of convective precipitation along the Gulf Coast in southern Mississippi and Alabama that was not occurring in observations was suppressed in the LDA run. An (albeit smaller) increase in grid-scale precipitation is evident in Figure 4 in the same area (bottom left), where some of the shallow convective precipitation is being produced.

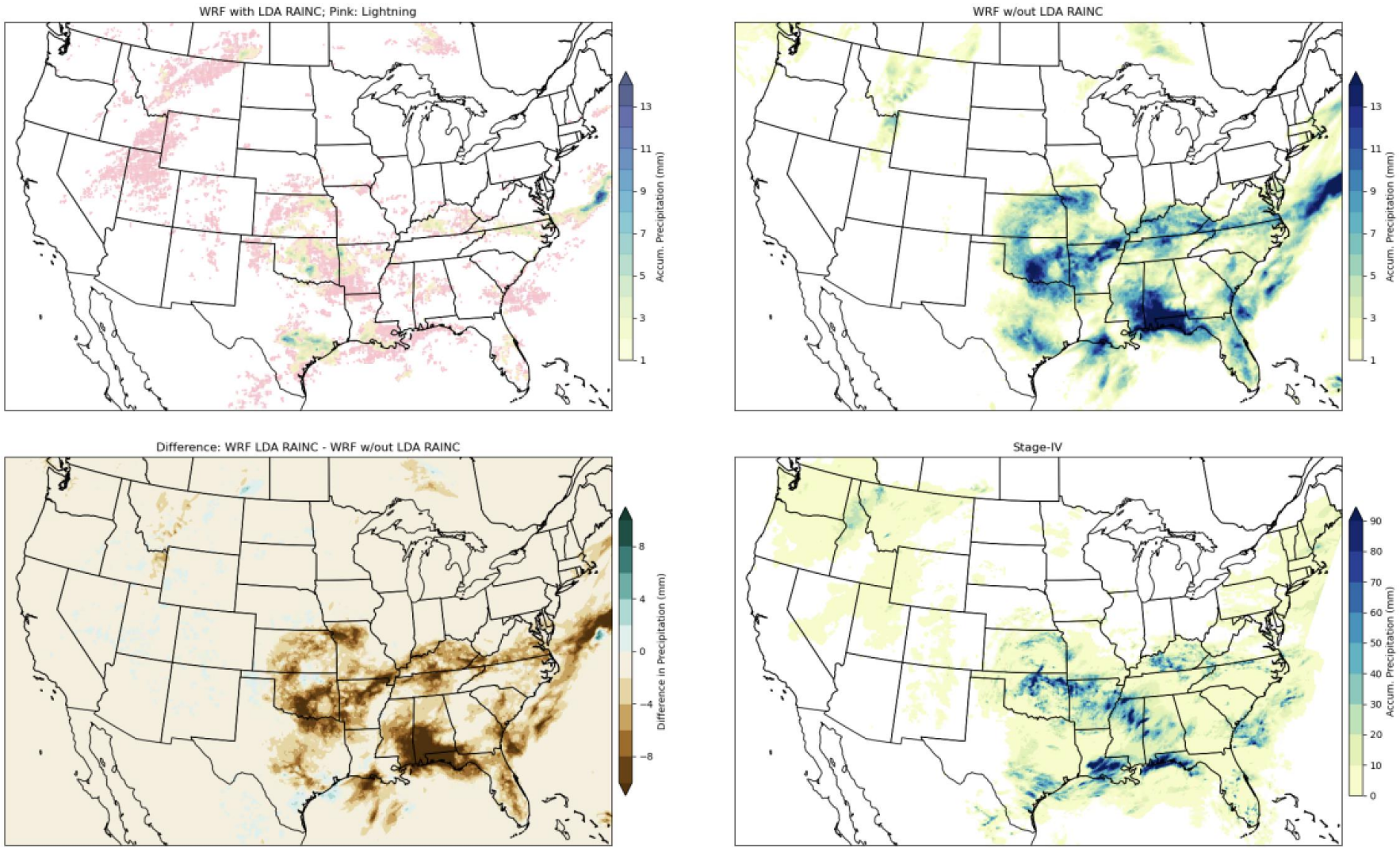

Figure 3: (upper left) WRF accumulated RAINC in LDA run (mm; colorbar) and occurrence of lightning in WRF grid cell (pink dots) over 24 h ending 0600 UTC 7 June 2019. (upper right) WRF accumulated RAINC in noLDA run (mm; colorbar). (bottom left) Difference between RAINC in LDA – noLDA run. Brown regions are where the LDA run was drier than the noLDA run. (bottom right) Stage-IV precipitation analysis. Note the different color scale used.

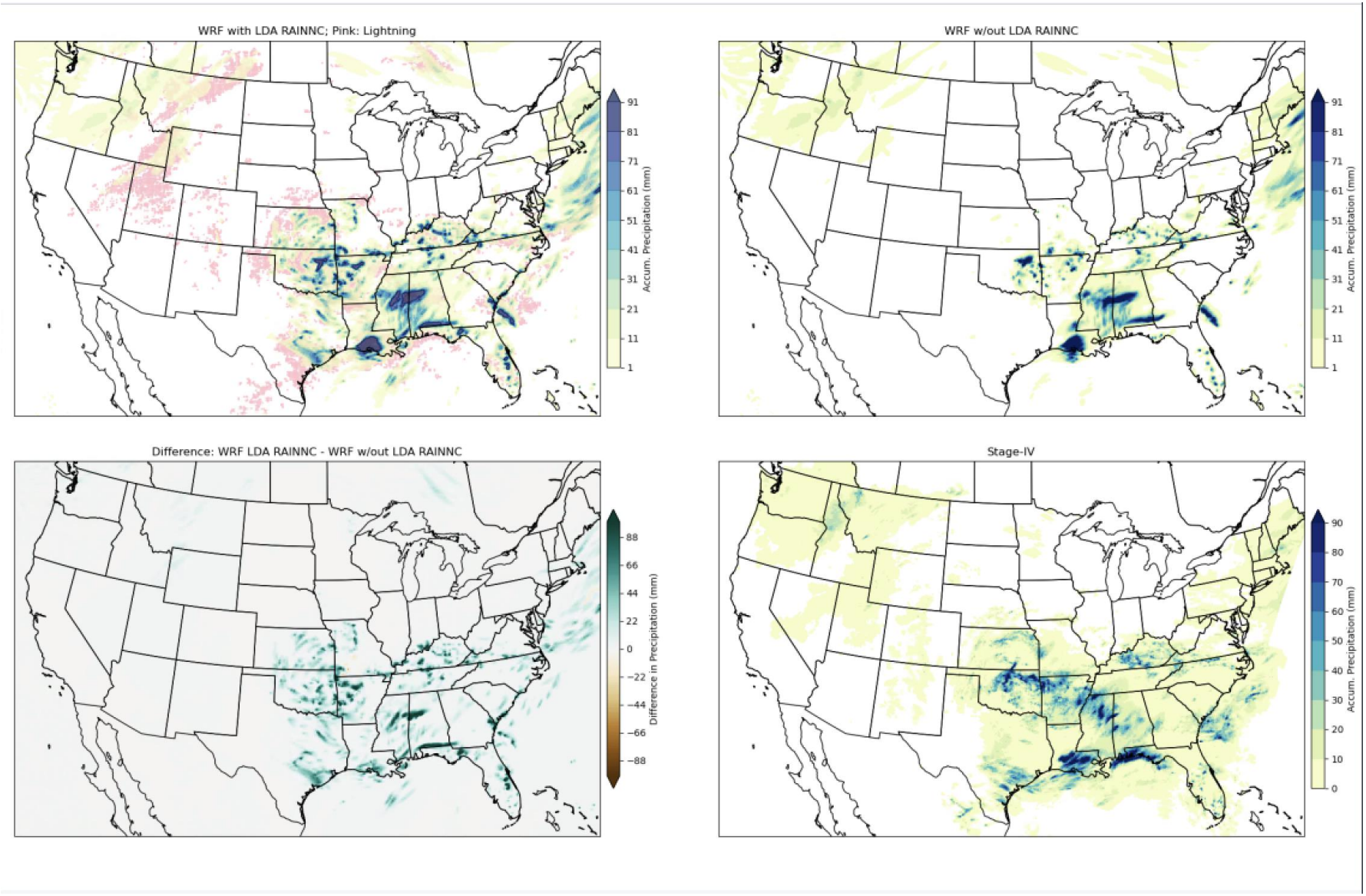

Figure 4: As in Fig. 2, but for RAINNC, gird-scale precipitation. Note the precipitation color scales for WRF RAINNC and Stage-IV are now similar.

However, unlike all AER's previous tests using LDA, the LDA did not result in an increase in RAINC in areas where lightning was occurring. Instead, it served only to suppress incorrect precipitation. Considering that the resulting forecast would be a good bit drier than the noLDA forecast, it is impressive the precipitation statistics showed little change.

The LDA design as well as a difference in entrainment calculation between the KF and Multi-Scale Kain Fritsch (MSKF) potentially reveals the answer for the lack of increase in RAINC. The LDA applies small perturbations in moisture and temperature to the cloud base within the parameterization's calculations of a convective updraft. If the resulting updraft is strong enough to reach the -20C level (as would be necessary to generate enough mixed phase particles for lightning to occur), the parameterization continues as normal. If the resulting updraft is not strong enough, additional moisture and temperature perturbations are applied until a limit of 1 g/kg of moisture increase has been applied. If the updraft is still not deep enough, no convection is trigged at that timestep, despite lightning having been present. This design is the same between the KF and MSKF configurations.

The potential difference lies in the calculation of the entrainment, and hence, updraft speed, in KF as compared to the MSKF. The MSKF includes an additional scaling factor when calculating entrainment that is dependent on the grid scale (i.e., Eqs. 1-3 of Zheng et al. 2016), that is not present in the KF. We theorize that this additional factor results in a different updraft profile. Thus, the perturbations applied by the LDA were only rarely able to produce a tall enough updraft to reach -20C. We hypothesize that increasing the perturbation limit of 1 g/kg of moisture would improve the LDA simulations by allowing it to force precipitation more successfully.

4 Impact of LDA on CAMx

4.1 Description of CAMx

To test the impact of the new MSKF LDA data assimilation on simulations of O_3 in Texas, we ran CAMx with (LDA) and without LDA (noLDA) for June 2019. CAMx inputs for May 15-June 30 were provided by TCEQ corresponding to their 2019 O_3 modeling platform, with a 12 km resolution over the contiguous US and a 4 km resolution over East Texas. We used wrf2camx to prepare updated 12 km and 4 km meteorological files to drive CAMx starting June 1 based on the WRF simulations discussed in Section 3.

Initial testing found an error in the wrf2camx land use files. These files lacked the "watermask" variable to distinguish fresh water from sea water. As the TCEQ inputs were in netCDF, and the watermask code provided by Ramboll only works on CAMx binary input files, we decided to use the TCEQ-provided land use files in our simulations. Thus, the only difference between the noLDA and LDA runs were the 4 km and 12 km 2D and 3D meteorological files.

4.2 Evaluation of CAMx with and without WRF LDA

Our CAMx runs were evaluated using AMET v1.3 and 2019 AQS data provided by the U.S. EPA[1]. Only the 4 km domain was evaluated as this would be of most interest to TCEQ. Here we discuss

[1] https://drive.google.com/drive/folders/1k37U9USjp6_vpr77BCyZ_JrxGtLudRWG from https://www.epa.gov/cmaq/atmospheric-model-evaluation-tool

the results for MDA8 O_3 at all sites in the 4 km domain. This evaluation satisfies the requirement that 10% of the data for the project be audited.

Table 5 shows various statistics for the CAMx runs with LDA and without LDA. In general, both model runs compare well to observations, with low mean bias and mean error. However, there is little difference between the noLDA and LDA runs, and to the extent there is a difference, the noLDA runs are slightly worse. For example, the mean bias across all East Texas sites and days increased to 2.5 ppbv from 2.2 ppbv when LDA was implemented.

Figure 5 shows a scatter plot of the MDA8 O_3 value at each site and day, (a) for LDA and (b) for noLDA. Figure 6 is a map of mean bias in MDA8 O_3 at each site in East Texas for June 2019. Again, there is little noticeable difference between the LDA and noLDA runs.

Table 5. Statistics for MDA8 O_3 across all sites in East Texas for June 2019.

Simulation	LDA	NoLDA
Mean Bias (ppb)	2.5	2.2
Mean Error (ppb)	9.3	9.2
RMSE (ppb)	11.6	11.3
Normalized Mean Bias (%)	6.1	5.4
Normalized Mean Error (%)	22.7	22.4
R^2	0.45	0.46

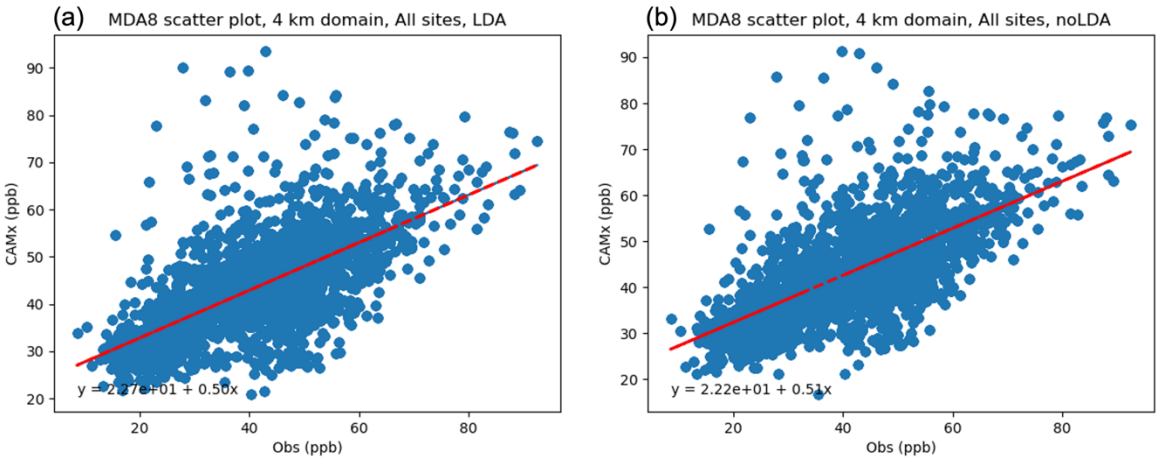

Figure 5. Scatterplots of MDA8 values for all days and sites in East Texas for June 2019. (a) a) CAMx simulation with LDA. (b) CAMx simulation without LDA.

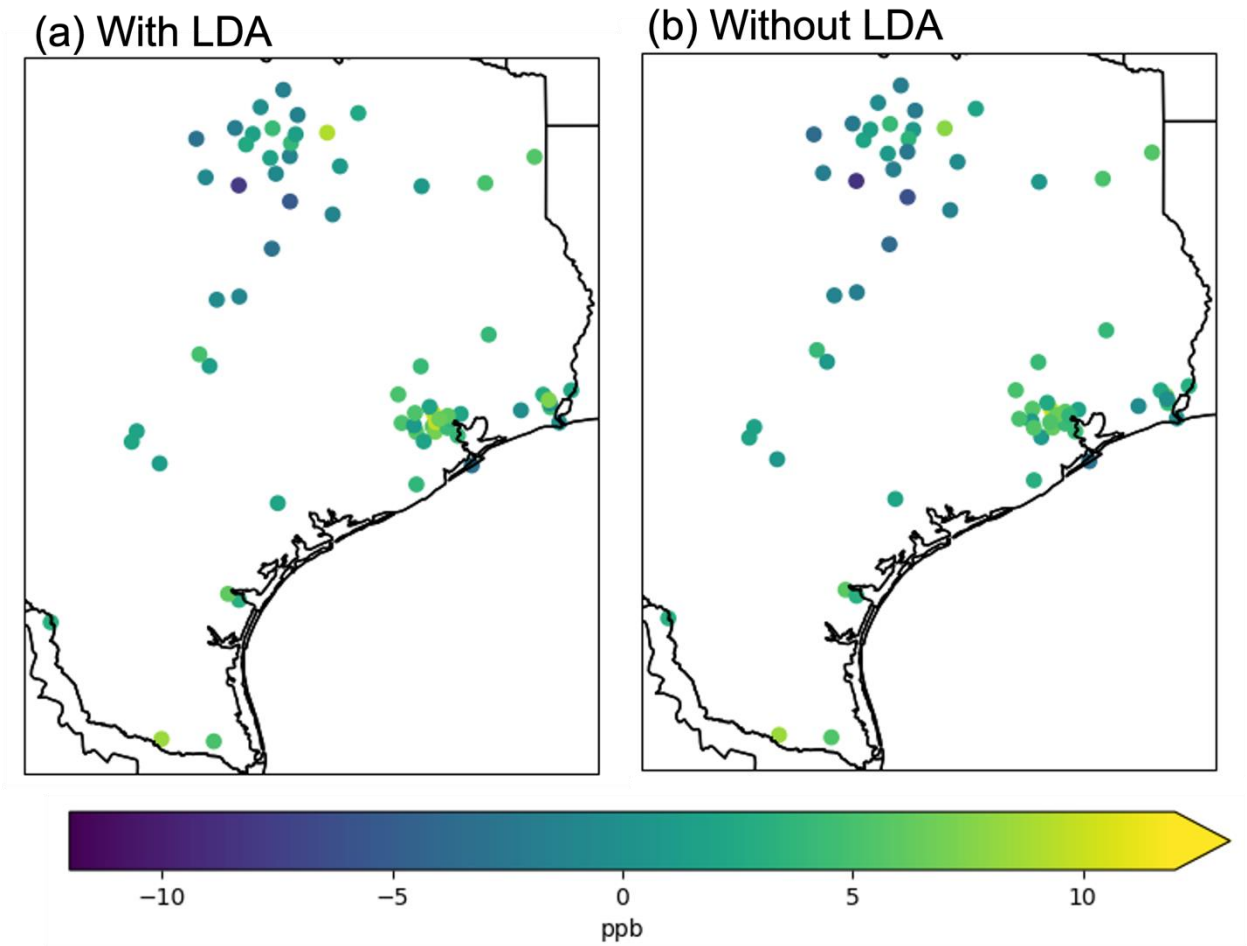

Figure 6. Mean bias in MDA8 O_3 for June 2019 at all AQS sites in East Texas. (a) CAMx simulation with LDA. (b) CAMx simulation without LDA.

5 Summary and Recommendations for Further Study

In this work, AER developed software to download, process, and regrid publicly available observations from the Geostationary Lightning Mapper (GLM) into the input format required by the WRF LDA method. A User's Guide was provided to TCEQ for this software. To determine the accuracy of the lightning regridding software, we (1) used multiple calculation methods to determine the WRF grid point nearest a flash and (2) plotted comparisons of multiple time periods of raw flash data and regridded data. Plots of co-located raw flash and regridded lightning data were also used for evaluation over different time scales (multiple days, multiple hours, only 10 minutes).

We implemented the LDA method into the Multi-Scale Kain-Fritsch (MSKF) scheme in WRF and provided TCEQ with a recipe to implement this change in current and future versions of WRF. We evaluated the performance of WRF for June 2019 simulations with the Model Evaluation Toolkit (MET). We found little difference in the temperature, wind, and precipitation verification across both domains, which was highly surprising. Evaluation revealed that the LDA worked almost solely to suppress precipitation where lightning did not occur and was not adding

precipitation where lightning was occurring. We theorize increasing the perturbation threshold LDA allows inside the MSKF to trigger convection could address this issue.

To test the impact of the new MSKF LDA data assimilation on simulations of O_3 in Texas, we ran CAMx with (LDA) and without LDA (noLDA) for June 2019. In general, both CAMx runs compare well to observations, with low mean bias and mean error. However, there is little difference between the noLDA and LDA runs, and to the extent there is a difference, the noLDA runs are slightly worse.

For future work, we suggest rerunning a few select dates from the "wet" subset of dates using an increased temperature and moisture perturbation threshold in the LDA option within MSKF.

6 References

Foroutan, H., and Pleim, J. E. (2017), Improving the simulation of convective dust storms in regional-to-global models*, J. Adv. Model. Earth Syst.,* 9, 2046– 2060, doi:10.1002/2017MS000953.

Goodman, S. J., and Coauthors (2013), The GOES-R Geostationary Lightning Mapper (GLM). *Atmos. Res.*, 125–126, 34–49, doi:https://doi.org/10.1016/j.atmosres.2013.01.006.

Heath, N. K., and D. Dean (2018), *Application of Lightning Data Assimilation Technique to Improve Transport and Dispersion Simulations*. Paper presented at 20th Joint Conference on the Applications of Air Pollution Meteorology with the A&WMA, American Meteorological Society, P6.4.

Heath, N. K., Pleim, J. E., Gilliam, R. C., and Kang, D. (2016), A simple lightning assimilation technique for improving retrospective WRF simulations, *J. Adv. Model. Earth Syst*., 8, 1806–1824, doi:10.1002/2016MS000735.

Holle, R. L., Cummins, K. L., and Brooks, W. A. (2016). Seasonal, Monthly, and Weekly Distributions of NLDN and GLD360 Cloud-to-Ground Lightning, *Mon. Wea. Rev*., 144(8), 2855-2870.

Kain, J. S,, (2004), The Kain-Fritsch convective parameterization: an update, J. Appl. Meteor. Climatol., 43(1), 170 -181., https://doi.org/10.1175/1520-0450(2004)043%3C0170:TKCPAU%3E2.0.CO;2

Kang, D., Mathur, R., Pouliot, G.A. et al. (2020), Significant ground-level ozone attributed to lightning-induced nitrogen oxides during summertime over the Mountain West States. *npj Clim Atmos Sci*, 3, 6 (2020). https://doi.org/10.1038/s41612-020-0108-2.

Kang, D., K. Pickering, D. Allen, K. Foley, Cheung Wong, R. Mathur, and S. Roselle (2019), Simulating lightning NO production in CMAQv5.2: evolution of scientific updates. *Geosci. Model Dev.*, Copernicus Publications, Katlenburg-Lindau, Germany, 12(7):3071–3083, (2019). https://doi.org/10.5194/gmd-12-3071-2019.

Pleim, J. E., Ran, L., Appel, W., Shephard, M. W., and Cady-Pereira, K. (2019), New bidirectional ammonia flux model in an air quality model coupled with an agricultural model. *J. Adv. Model. Earth Sys.*, 11, 2934– 2957. https://doi.org/10.1029/2019MS001728.

Pye H. T., Zuend A, Fry JL, et al. (2018), Coupling of organic and inorganic aerosol systems and the effect on gas-particle partitioning in the southeastern US. *Atmos Chem Phys*., 18(1), 357-370. doi:10.5194/acp-18-357-2018

Zheng, Y., Alapaty, K., Herwehe, J. A., Del Genio, A. D., and Niyogi, D. (2016). Improving High- Resolution Weather Forecasts Using the Weather Research and Forecasting (WRF) Model with an Updated Kain–Fritsch Scheme, *Mon. Wea. Rev.*, 144(3), 833-860